8

Solution Conformation of a Pectic Acid Fragment by ^{1}H-NMR and Molecular Dynamics

A. DI NOLA,[1] G. FABRIZI,[2] D. LAMBA,[3] and A. L. SEGRE[3,*]

[1]Dipartimento di Chimica, Università di Roma "La Sapienza," P. le A. Moro 5, I-00185 Roma; [2] Dipartimento di Chimica, Ingegneria Chimica e Materiali, Università dell'Aquila, Via Assergi, 6, I-67100 L'Aquila; and [3]Istituto di Strutturistica Chimica "Giordano Giacomello," Area della Ricerca di Roma, CNR, C.P. no. 10, I-00016 Monterotondo Stazione, Roma, Italy

SYNOPSIS

^{1}H-NMR and molecular dynamics simulations in vacuo and in water of (1 → 4)-α-D-galacturono-disaccharide were performed. The results of the molecular dynamics simulations showed that the molecule fluctuates between two conformations characterized by different values of torsion angles around the glycosidic linkage and two different intramolecular hydrogen bonds. When these conformations are extrapolated to a regular polymeric structure, they generate pectic acid compatible with a 2_1- or a right-handed 3_1-helix. © 1994 John Wiley & Sons, Inc.

INTRODUCTION

Oligosaccharides were studied, both experimentally and theoretically, due to the fact that they are considered model compounds for polysaccharides. One of the most important points to consider concerns the conformation and fluctuations of the glycosidic torsion angles that are sensitive to pH variations, ionic strength, hydration, and counterions. These are all importants features that determine the folding of the polymer.

Most of the molecular mechanics calculations were performed in vacuo[1,2]; more recently molecular dynamics (MD) simulations of carbohydrates in aqueous solution have been performed[3–6] and highlighted the nature and role of hydrogen bonding in model carbohydrate solutions.[6]

In the present paper we have reported the results of an nmr and MD study in solution of the model compound (1 → 4)-α-D-galacturono-disaccharide. It is worth noting that the pectin molecule has its principal component α-D-Gal*p*A present in linear (1 → 4)-linked conformation.[7]

The use of MD simulations can show the effect of conformational transitions and the nature of normal structural fluctuations. Moreover, with this technique the solvent can be introduced so that water molecules can be included in the computation.

The aim of this study is to elucidate the conformation and fluctuations of the glycosidic linkage of the dimer, which is still a matter of dispute. In the polymer, in fact, different ions seem to stabilize different conformations and both 2_1- and 3_1-helices have been suggested by x-ray and molecular modeling.[8–13]

Conformational transitions have been suggested by CD,[14] calorimetric measurements,[15] and EXAFS investigations[16] of solid and gel forms of calcium poly(α-D-galacturonate).

Recently Hricovíní et al. have reported a study based on nmr and molecular mechanics in vacuo and with a continuum model evaluating the effect of the solvent,[17] suggesting a right-handed 3_1-helical arrangement formed by pectic acid oligosaccharides. However, in the case of pectins, both right- and left-handed single-stranded helices along with a 2_1-helix have also been suggested.[18]

The question as to how the molecule can fluctuate among different conformations can be addressed with molecular dynamics and will be rationalized in the present paper.

Biopolymers, Vol. 34, 457–462 (1994)

CCC 0006-3525/94/040457-06

* To whom correspondence should be addressed.

METHODS

(1 → 4)-α-D-Galacturono-Disaccharide

The title compound was purchased from Sigma and used without further purification.

Nomenclature

The recommendations and symbols proposed by the Commission on Nomenclature[19] are used throughout this paper. A schematic drawing of the disaccharide, along with the labeling of the atoms of the MD simulation, is given in Figure 1. The relative orientation of a pair of contiguous residues around the glycosidic linkage is described by a set of two torsional angles:

$$\phi = O5' — C1' — O1' — C4$$

$$\psi = C1' — O1' — C4 — C5$$

The orientation of the two carboxylic moieties is described by the torsion angles:

$$\chi = O5 — C5 — C6 — O6A$$

$$\chi' = O5' — C5' — C6' — O6'A$$

NMR Spectroscopy

All spectra were recorded on a Bruker AM-400. The ^{1}H-NMR spectrum (400.13 MHz) of a solution of **1** in D_2O (1 mg/mL) at 298 K (pD = 2.75, internal acetone, 2.225 ppm) indicated an $\alpha : \beta$ ratio of 40 : 60. Peak assignments were performed by double quantum filtered correlated spectroscopy (COSY) as described.[20–22] A nuclear Overhauser effect spectroscopy (NOESY)[23] spectrum was performed with a contact time of 800 ms.

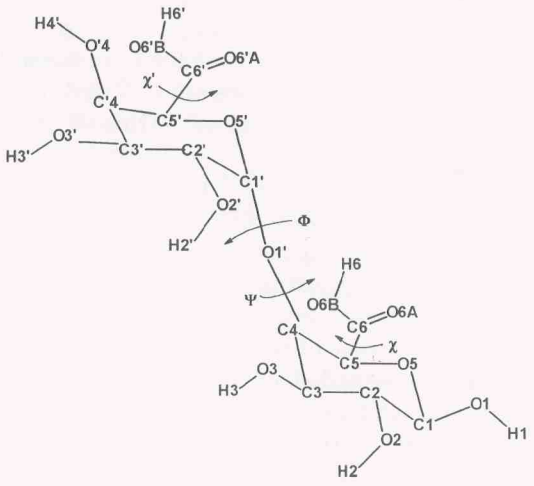

Figure 1. Scheme and atoms labeling of the (1 → 4)-α-D-galacturono-disaccharide.

MD Simulation

MD simulations in vacuo and in water were performed with programs from the *GR*oningen *MO*lecular *S*imulation system (GROMOS) software package.[24] The applied empirical potential energy function contains terms representing covalent bond stretching, bond angle bending, harmonic dihedral angle bending (out-of-plane, out-of-tetrahedral configuration), sinusoidal dihedral angle torsion, Van der Waals, and electrostatic interactions.[25] A dielectric permittivity, $\epsilon = 1$, was used. The cutoff radius for the nonbonded interactions was chosen in order to include all interactions for the simulation in vacuo, while 0.8 nm was used for the simulation in water.

The simulation in vacuo was performed with an attractive half-harmonic restraining potential to force the molecule to satisfy selected NOE distances[26]:

$$V_{DR}(d_{kl}) = 1/2K_{DR} \cdot (d_{kl} - d^*_{kl})^2 \quad \text{if } d_{kl} \geq d^*_{kl}$$

$$V_{DR}(d_{kl}) = 0 \quad \text{if } d_{kl} \leq d^*_{kl}$$

where K_{DR} is the force constant (10 kJ · mol^{-1} · Å^{-2}), d_{kl} is the distance between protons and d^*_{kl} is the reference distance. The energy increases for $d_{kl} \geq d^*_{kl}$; thus the added potential is attractive for $d_{kl} \geq d^*_{kl}$.

In order to translate the NOE information into distance ranges d^*_{kl}, upper limits of 0.3, 0.4, and 0.5 nm for strong, medium, and weak NOEs, respectively, were chosen.[27] Only hydroxylic hydrogens were explicitly treated.

Bond stretching terms were not included in the calculation; the SHAKE[28] algorithm was used to constrain bond lengths. The use of constant bond lengths in MD is widely used, saving computational time, as well as allowing a long time step, (by a factor of 2–3); it has also been proved[29] that this approximation does not modify physical and chemical properties.

The initial conformation of the MD simulation was a random one with the reducing end of the disaccharide molecule having the β configuration. All atoms were given an initial velocity obtained from

a Maxwellian distribution at the desired initial temperature. The rescaling of the temperature during the run was obtained by a coupling with an external bath,[30] with a time constant $\tau = 0.1$ ps. A time step of 0.002 ps was used in the simulation.

The search of the structure that accounts for the experimental NOEs was performed by the simulated annealing procedure,[31] based on a high temperature run followed by a slow cooling and equilibration. The restraining potential that accounts for experimental NOEs was applied during the whole simulation in vacuo.

A first 30 ps simulation in vacuo at $T = 800$ K was performed; then the simulated annealing was carried out in 50 ps with the final temperature at 300 K. The system was finally equilibrated at 300 K for 50 ps.

The conformer obtained by the simulated annealing procedure was placed in a periodic computational box containing 289 water molecules. The box was chosen to be a cubic one, the edge being 2.1 nm and a periodic boundary condition was applied. A cutoff radius of 0.8 nm was used. MD simulations were performed after the initial energy minimization of the water molecules, with no inclusion of the restraining potentials, at a constant pressure of 1 atm and at a constant temperature $T = 300$ K. The time step was 0.002 ps. The first 30 ps were used for equilibration; they were followed by 80 ps subsequently used for analysis.

The calculations were performed on the IBM 3090 of the University of Rome.

RESULTS AND DISCUSSION

NMR Spectra in D_2O

A complete analysis of the one-dimensional spectrum (chemical shift and coupling constants) is reported in Table I. It is worth noting the small differences in chemical shifts of the H5α and H5β protons in our study, compared with those reported by Hricovíni et al.,[17] which may be ascribed to the different pH of the solutions. NOESY cross peaks were divided into strong, medium, and weak. Intraring cross peaks and vicinal J coupling are consistent with an unperturbed $^4C_1$ conformation for the two residues. Some interring cross peaks were not considered because they were found to strongly overlap with COSY or to intraring cross peaks. However, two well-defined interring cross peaks are present in the disaccharides with either α or β configuration. Table IV reports those of the β anomer, which is the one used in the MD simulations.

Table I Assignment of Chemical Shift (ppm) and $^3J_{H\text{-}H}$ Coupling Constants from One-Dimensional Spectra of (1 → 4)-Linked α-D-Galacturono-Disaccharide Performed at 400.13 MHz

Proton	Chemical Shift	J	Proton	Chemical Shift	J
H1α	5.383		H1β	4.693	
		3.8			7.8
H2α	3.857		H2β	3.534	
		10.5			10.2
H3α	4.064		H3β	3.832	
		3.2			3.3
H4α	4.488		H4β	4.430	
		1.4			1.2
H5α	4.763		H5β	4.421	
H1′α	5.108		H1′β	5.103	
		4.0			3.9
H2′α	3.766		H2′β	3.760	
		10.6			10.5
H3′α	3.963		H3′β	3.988	
		3.4			3.4
H4′α	4.362		H4′β	4.368	
		1.8			1.8
H5′α	5.108		H5′β	5.108	

MD in Vacuo and in Water

At the end of the simulated annealing and during the last 50 ps of the simulation in vacuo at $T = 300$ K the molecule was found to lie in a well-defined conformation characterized by the expected $^4C_1$ conformation of the pyranoid rings (as reported in Table II), and by the presence of the O6′B—H6′ · · · O3 intramolecular hydrogen bond (as reported in Table III). The distances between the H4 · · · H1′ and H2 · · · H5′ protons agree with the experimental NOEs (see Table IV). The ϕ and ψ torsion angles have the average values 87.9° and 123.5° with rms fluctuations of 3.3° and 3.4°, respectively. The small fluctuations of distances and angles, reported in Tables II–IV, indicate that a rigid conformation is adopted in vacuo.

At the end of the simulation in vacuo the molecule was placed in a periodic computational box containing the water molecules, with no restraints for the H4 · · · H1′ and H2 · · · H5′ proton distances. The first 30 ps of the simulation were used for equilibration and the last 80 ps were used for analysis. Tables II–IV report the results obtained for torsion angles, hydrogen bonds, and NOEs. The molecule retains the $^4C_1$ conformation of the pyranoid rings (Table II) and the H4 · · · H1′ and H2 · · · H5′ proton distances (Table IV). Values for the torsion

Table II Average Torsion Angle Values of the Pyranoid Rings, with Their RMS Fluctuations, Obtained in the Last 50 ps of the MD Simulation in Vacuo and in the Simulation in Water at T = 300 K

Torsion Angle	MD Simulation in Vacuo	RMS Fluctuations	MD Simulation in Water	RMS Fluctuations
C1-C2-C3-C4	−59.4	2.0	−55.2	7.0
C2-C3-C4-C5	59.9	2.1	58.9	5.7
C3-C4-C5-O5	−59.9	2.1	−63.1	5.7
C4-C5-O5-C1	61.8	2.4	64.3	6.7
C5-O5-C1-C2	−60.4	2.7	−58.3	8.0
O5-C1-C2-C3	58.0	2.2	52.3	7.9
C1′-C2′-C3′-C4′	−55.3	2.3	−56.4	6.4
C2′-C3′-C4′-C5′	53.7	2.2	57.4	5.9
C3′-C4′-C5′-O5′	−54.8	1.9	−56.7	5.7
C4′-C5′-O5′-C1′	61.1	2.1	59.4	6.7
C5′-O5′-C1′-C2′	−60.0	2.1	−57.3	6.8
O5′-C1′-C2′-C3′	55.3	2.0	53.7	6.7

angles of the pyranoid rings are in good agreement with the J_{H-H} of the nmr experiment, but the $^4C_1$ conformation is slightly distorted, as described in Table II. All the secondary hydroxyls are in continuous rotation during the simulation in water and are hydrogen bonded with the solvent. It is worth noting that throughout the whole simulation time, the two carboxyls show small fluctuations of the torsion angles χ and χ', 43.9 (13.4)° and −136.6 (12.5)°, respectively.

Tables II and IV show that the rms fluctuations in water are at least three times greater than those in vacuo, so that the conformation in water is more flexible.

It should be noted that (see Table IV) the H4 · · · H1′ and H2 · · · H5′ proton distances both in vacuo and in water simulations well agree with those derived from the experimental NOE data.

It is interesting to follow the history of the ϕ and ψ torsion angles in water as shown in Figure 2. This highlights a strong correlation between the two angles and it shows that the simulation can be divided into three time intervals: 30–50, 50–80, and 80–110 ps. In the first and last interval the ϕ and ψ angles fluctuate around well-defined values: ϕ_1 = 90.2 (6.1)°, ψ_1 = 130.4 (6.9)°, ϕ_3 = 127.5 (10.0)°, and ψ_3 = 152.7 (8.1)°. In the 50–80 ps interval the molecule experiences a transition from 1 to 3. These ϕ and ψ values are closely related to the intraresidue hydrogen-bond formation. In fact, analysis of the hydrogen-bond occurrence (Table III) shows the presence in water of either the O6′B—H6′ · · · O3 hydrogen bond in the 30–50 ps interval (see Figure 3a), or the O2′B—H2′ · · · O6B hydrogen bond in the 80–110 ps interval (see Figure 3b). The former has also been observed in vacuo. The temporary disruption of intramolecular hydrogen bonds in carbohydrates system has already been observed for maltose in aqueous solution.[6]

Table V lists the average energies and standard deviations of the mean obtained by accounting for statistical correlation of the data by the method of Straatsma et al.[32] Table V reports the solute/solute, solute/water, and total potential energies of the solute. It can be seen that the solute/solute energy is significantly lower in the 30–50 ps interval than in the 80–110 ps interval, whereas the solute/water energy is significantly lower in the 80–110 ps interval than in the 30–50 ps interval. The total potential energy of the solute is exactly the same in the 30–

Table III Occurrence (Percentage of Time) of Intramolecular Hydrogen Bonds During the Last 50 ps of the Simulation in Vacuo at T = 300 K and During the Simulation in Water[a]

MD Simulation	H-Bond O6′B—H · · · O3	H-Bond O2′—H · · · O6B
Vacuo	100	0
Water 30–50 ps	97	0
Water 50–80 ps	31	2
Water 80–110 ps	0	90

[a] Characteristics of the hydrogen bonds: (1) O6′B—H · · · O3 donor (D) · · · acceptor (A) average distance 0.28 nm, D—H · · · A angle 159°; (2) O2′—H · · · O6B D · · · A average distance 0.27 nm, D—H · · · A angle 162°.

Table IV NOE Effects Observed in the NOESY Spectra[a]

NOE NMR	NMR Intensity	MD Average Distance in Vacuo (v)	RMS Fluctuations	MD Average Distance in Water (v)	RMS Fluctuations
H4 · · · H1′	Strong	0.181	0.007	0.182	0.017
H2 · · · H5′	Medium	0.304	0.012	0.332	0.050

[a] Average internuclear distances (nm) and rms fluctuations (nm) obtained in the last 50 ps of the MD simulation in vacuo at T = 300 K and in the simulation in water.
v: Virtual atom.

50 and 80–110 ps intervals (i.e., when intramolecular hydrogen bonds occur) and slightly lower in the 50–80 ps interval. The values of the total potential energies of the solute in the different conformations show that all the conformers are allowed at 300 K, the potential energy differences between conformers I–II and II–III being within 3 times their rms.

CONCLUSION

The MD simulation in vacuo shows a conformation which corresponds to the lowest energy minimum found by Hricovíni et al.[17] in the relaxed (ϕ, ψ) map computed by the MM2CARB[33] force field. Furthermore, Cros et al.[18] have shown that the analogous map computed by the MM3[34,35] force field for the 4-O-α-D-galactopyranurosyl-1-O-methyl α-D-galactopyranuronic 6,6′-dimethyl diester is similar to the one computed for the acidic disaccharide.

This conformation is consistent with the nmr data and it is characterized by the presence of an intramolecular O6′B — H6′ · · · O3 hydrogen bond, not brought to light by the above-mentioned molecular mechanics studies.

The most striking feature of the MD simulation in water is the occurrence of two energetically equivalent conformers: one corresponds to that observed in the MD simulation in vacuo, the other is characterized by the O2′B — H2′ · · · O6B intramolecular hydrogen bond.

When extrapolated to a regular polymeric structure, these conformations generate different arrangements: conformer 3 gives pectic acid with a twofold 2_1-helix; conformers 1 and 2 give pectic acid

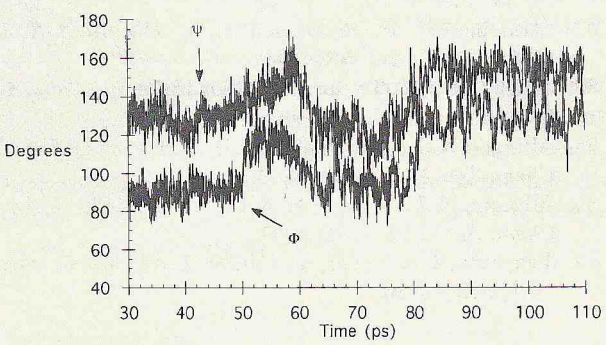

Figure 2. Time course of the glycosidic ϕ and ψ torsion angles over the 30–110 ps MD simulation in water.

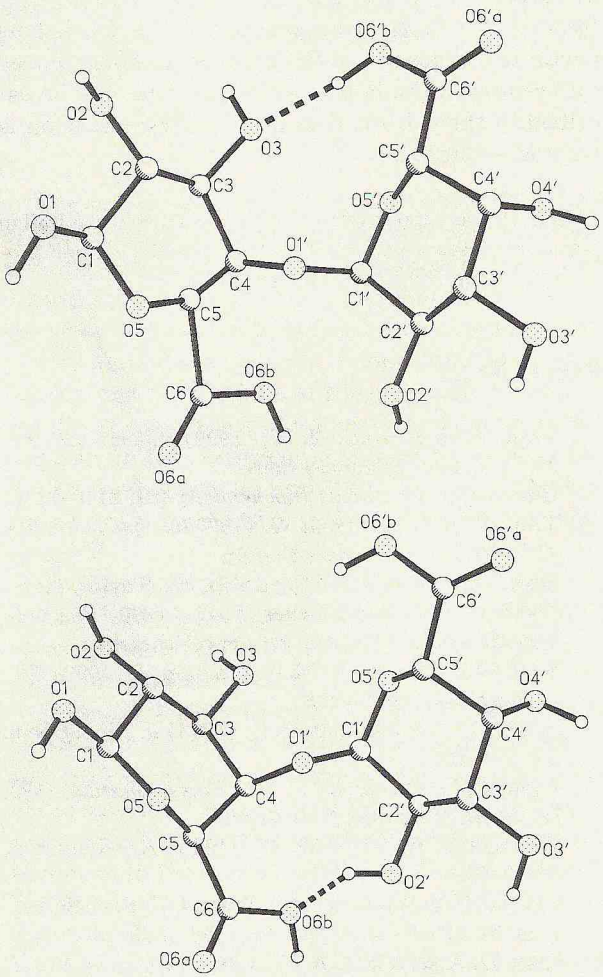

Figure 3. Average structures over the 30–50 ps (a) and 80–110 ps (b) of the MD simulation in water showing the intramolecular hydrogen bonds.

Table V Time-Averaged Potential Energies of the Solute and Standard Deviations in Aqueous Solution (kJ · mole^{-1})

MD Simulation (ps)	$E_{solute/solute}$	$E_{solute/water}$	E_{tot}
Water 30–50	410 ± 6	−521 ± 17	−111 ± 14
Water 50–80	470 ± 9	−610 ± 8	−140 ± 10
Water 80–110	473 ± 5	−583 ± 12	−109 ± 8

close to a threefold 3_1 right-handed helix. Nevertheless, the (ϕ, ψ) relaxed map indicates that both right- and left-handed single-stranded helices may occur, along with a 2_1-helix, without drastic conformational changes.[17,18] Of certain interest is the conclusion that MD simulation in water is not consistent with the results from molecular mechanics calculations,[17] which use a continuum model to evaluate the effect of solvent[36] and which suggests that only a right-handed 3_1-helical arrangement can be formed by pectic acid oligosaccharides in solution. The reported differences in the helical arrangements may be ascribed to the solvent that in the MD simulation is treated explicitly.

This work was supported in part by grants from the Italian National Research Council (CNR), special ad hoc programme "Chimica fine II" subproject 3.

REFERENCES

1. Tran, V. H. & Brady, J. W. (1990) *Biopolymers* **29**, 961–976, and references therein.
2. Homans, S. W. (1990) *Biochemistry* **29**, 9110–9118.
3. Tran, V. H. & Brady, J. W. (1990) *Biopolymers* **29**, 977–997, and references therein.
4. Edge, C. J., Singh, U. C., Bazzo, R., Taylor, G. L., Dwek, R. A. & Rademacher, T. W. (1990) *Biochemistry* **29**, 1971–1974, and references therein.
5. Kroon-Batenbourg, L. M. J. & Kroon, J. (1990) *Biopolymers* **29**, 1243–1248.
6. Brady, J. W. & Schmidt, R. K. (1993) *J. Phys. Chem.* **97**, 958–966.
7. Aspinall, G. O. (1985) in *The Polysaccharides,* Vol. III, Academic Press, New York.
8. Wuhrmann, K. & Pilnik, W. (1945) *Experientia* **1**, 330–332.
9. Palmer, K. J., Merrill, R. C., Owens, H. S. & Ballantyne, M. (1947) *J. Phys. Chem.* **51**, 710–720.
10. Rees, D. A. & Wight, A. W. (1971) *J. Chem. Soc. B* 1366–1372.
11. Sathyanarayana, B. K. & Rao, V. S. R. (1973) *Curr. Sci. B* 1366–1372.
12. Gould, S. E. B., Gould, R. O., Rees, D. A. & Wight, A. W. (1976) *J. Chem. Soc. Perkin II,* 392–398.
13. Walkinshaw, M. D. & Arnott, S. (1981) *J. Mol. Biol.* **153**, 1055–1073.
14. Morris, E. R., Powell, D. A., Gidley, M. J. & Rees, D. A. (1982) *J. Mol. Biol.* **155**, 507–516.
15. Cesaro, A., Ciana, A., Delben, F., Manzini, G. & Paoletti, S. (1982) *Biopolymers* **21**, 431–449.
16. Alagna, L., Prosperi, T., Tomlinson, A. A. G. & Rizzo, R. (1986) *J. Phys. Chem.* **90**, 6853–6857.
17. Hricovíni, M., Bystricky', S. & Malovíková, A. (1991) *Carbohydr. Res.* **220**, 23–31.
18. Cros, S., Hervé du Penhoat, C., Bouchenal, N., Ohassan, H., Imberty, A. & Perez, S. (1992) *Int. J. Biol. Macromol.* **14**, 313–320.
19. IUPAC-IUB Commission on Biochemical Nomenclature. (1971) *Arch. Biochem. Biophys.* **145**, 405–421.
20. Piantini, U., Sorenson, O. W. & Ernst, R. R. (1982) *J. Am. Chem. Soc.* **104**, 6800–6801.
21. Shaka, A. J. & Freeman, R. (1983) *J. Magn. Reson.* **51**, 169–173.
22. Rance, M., Sorenson, O. W., Bodenhausen, G., Wagner, G. & Ernst, R. R. (1984) *Biochem. Biophys. Res. Commun.* **117**, 479–485.
23. Bodenhausen, G., Kogler, H. & Ernst, R. R. (1984) *J. Magn. Res.* **58**, 370–388.
24. van Gunsteren, W. F. & Berendsen, H. J. C. (1987) *Groningen Molecular Simulation (GROMOS) Library Manual,* Biomos, Groningen.
25. Åqvist, J., van Gunsteren, W. F., Leijonmarck, M. & Tapia, O. (1985) *J. Mol. Biol.* **183**, 461–477.
26. Kaptein, R., Zuiderweg, E. R. P., Scheek, R. M., Boelens, R. & van Gunsteren, W. F. (1985) *J. Mol. Biol.* **182**, 179–182.
27. Kaptein, R., Boelens, R., Scheek, R. M. & van Gunsteren, W. F. (1988) *Biochemistry* **27**, 5389–5395.
28. Ryckaert, J. P., Ciccotti, G. & Berendsen, H. J. C. (1977) *J. Comput. Phys.* **23**, 327–341.
29. Karplus, M. & Van Gunsteren, W. F. (1982) *Macromolecules* **15**, 1528–1544.
30. Berendsen, H. J. C., Postma, J. P. M., van Gunsteren, W. F., Di Nola, A. & Haak, J. R. (1984) *J. Chem. Phys.* **81**, 3684–3690.
31. Kirkpatrick, S., Gelatt, C. D., Jr. & Vecchi, M. P. (1983) *Science* **220**, 671–680.
32. Straatsma, T. P., Berendsen, H. J. C. & Stam, A. J. (1986) *Mol. Phys.* **57**, 89–95.
33. Jeffrey, G. A. & Taylor, R. (1980) *J. Comp. Chem.* **1**, 99–109.
34. Allinger, N. L., Yuh, Y. H. & Lii, J.-H. (1989) *J. Am. Chem. Soc.* **111**, 8551–8556.
35. Allinger, N. L., Yuh, Y. H. & Lii, J.-H. (1990) *J. Am. Chem. Soc.* **112**, 8293–8307.
36. Tvaroska, I. & Kozár, T. (1980) *J. Am. Chem. Soc.* **102**, 6929–6936.

Received March 8, 1993
Accepted August 16, 1993